

EFFECT OF LOW VELOCITY IMPACT DAMAGE ON THE BUCKLING BEHAVIOUR OF COMPOSITE PANELS

G. Romeo*, G. Gaetani**

* Politecnico di Torino, Dept. of Aerospace Engineering, Turin, Italy.

** Aeronautic High School "C. Grassi", Turin, Italy.

Abstract

The effect of impact damage on the buckling behaviour of advanced composite panels is one of the most featuring subjects in designing aerospace structures. The drop mass test method (2.76 kg mass and velocity up to 6.5 m/sec, corresponding to an impact energy up to 58 J) was used. The damage morphology is very much influenced, besides impact energy, by the clamping system of the panel during the impact test. Impact damage was measured nondestructively by C-scan ultrasonic system using a 15 MHz transducer; a destructive technique was used to study impact damage distribution through the thickness. Several panels were tested to inplane shear or uniaxial compression load to verify the effect of the damage on the buckling load; with respect to the non impacted panels, buckling load reduction up to 30% was obtained for panels impacted up to 41 Joule. Specimens tested under shear load failed at applied loads that are 3 or 4 times larger than the buckling load; however, specimens tested under compression load failed at applied loads that are 2 times higher than the buckling load.

1. Introduction

Analytical and experimental results on the structural efficiency of aerospace structures under compression and shear loads have demonstrated the mass-saving potential of advanced composite panels to meet buckling requirements. However, an important consideration in attaining these potential improvements is the need to know the resistance of composite materials to impact damage which may occur in normal service (debris, hailstones, etc.) or for tool drop. The impact resistance of graphite epoxy structures is much lower than that of aluminium structures; furthermore, the damage is not visible from the impact side when the impact energy is lower certain values.

The damage propagation mechanism for laminated composites was noted to be dependent upon the position of the delaminated region with respect to the laminate surface⁽¹⁾; the closer the delaminations are to the surface, the lower is the load required to initiate local buckling.

2. Impact Damage Test Techniques

Two different test techniques are used in the laboratories to impact laminated composites. The first one, widely used in the industries, is the dropped mass test method and is conducted in the following manner. A high mass impactor, up to 4.5 kg, have a hemispherical steel tip with diameter up to 2 cm and length up to 25 cm; specimens are clamped, or supported, along edges between two steel plates having 4 cm central hole or wider rectangular shape; the mass is then dropped from a height up to 2 m or more and strikes the specimen normal to its plane at speed up to 6.5 m/sec or more (see Fig.1). Impactor are usually instrumented by a semiconductor strain gage transducer, mounted in the tip, to measure the contact force as function of time; the elastic deformation of the impactor during the impact is elaborated by computer to determine the contact force $F(t)$ and, sequentially, acceleration $a(t)$, velocity during the contact $V(t)$, impactor displacement $X(t)$ and impact energy $E(t)$. It is very important to measure both contact force and impact energy directly on the specimen.

The second method used by NASA to impose impact damage involves propelling a small mass (1.27 cm diameter aluminium sphere) at speed up to 150 m/sec; this test, infact, is considered more similar to impact damage which may occur in normal service. Damage test was conducted in the same fixture used to carry out the compression test⁽²⁾.

Although identical impact energies is imposed on the specimens, results obtained showed considerably larger damage size for NASA test method compared to that for dropped mass method. The main reason for such difference was explained as effect of a local out-of-plane deformation gradient, which occur in a time much less than that required for the overall response of the plate structure, producing larger transverse shear and failure within the laminate.

The drop mass test method is influenced by the edge support boundary condition (clamped or simply supported); furthermore, it is affected by the dimensions of the plate; infact, if the panel is clamped between plates having a 4 cm central hole the damage size is limited just to this dimension; indeed, a different damage size is possible when the panel is fixed in a

rectangular frame with a wider clamped area

Some experimental tests were carried out for first on small specimens impacted at different impact energy levels by the dropped mass test method. A 2 cm diameter steel impactor (having a 1.5 kg mass) was used to impact the center of a BASF T800/5245C graphite/bismaleimide plate $[45_2/-45_2/0_2/90_2]_s$ having a total thickness of 1.85 mm; the size of the plate is 6 cm by 6 cm and is clamped between two plates having a 4 cm central hole. Five specimens were impacted at different velocities and energies as reported in Table 1.

Specimen	1	6	7	10	13
Velocity [m/sec]	2.5	3.5	4.5	5.5	6.5
Energy [J]	4.6	9.1	14.3	20.5	27.4

TABLE 1 IMPACT TEST ON SMALL SPECIMENS

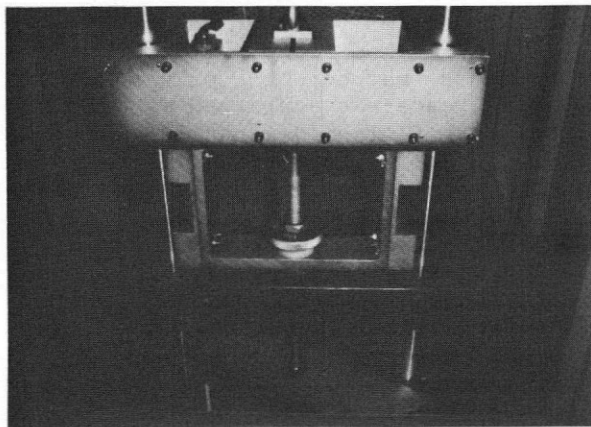
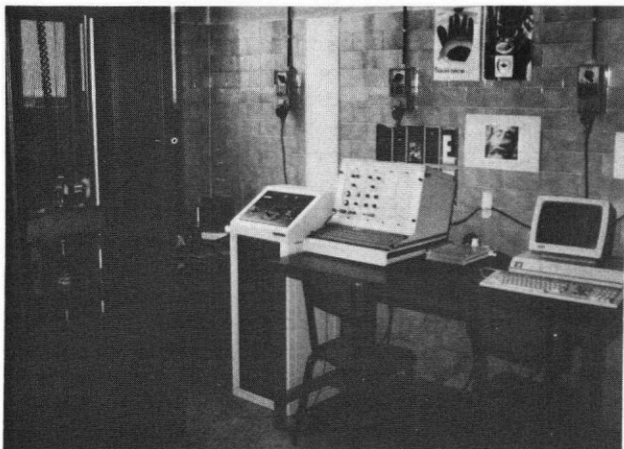


FIG.1- DROPPED MASS TEST EQUIPMENT

Specimens were cross-sectioned through the impacted region for a microscopical observation of interior damage. Visual inspection showed front and back surface damage for each specimen although the back damage was much wider than front damage (see Fig. 2); photomicrographs of the cross section of specimen 1 in the damaged region is shown in Fig.2a; it exhibit delamination cracks between plies of dissimilar orientation (specially in the back surface between +45 and -45) as well as through the thickness cracking of 0 and + or -45 oriented plies assuming a typical V-shaped pattern. For higher values of impact energy a wider and catastrophic damage area was observed.

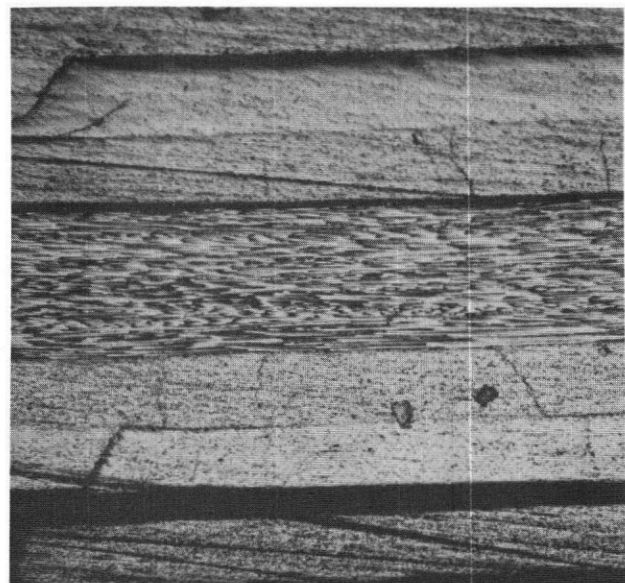
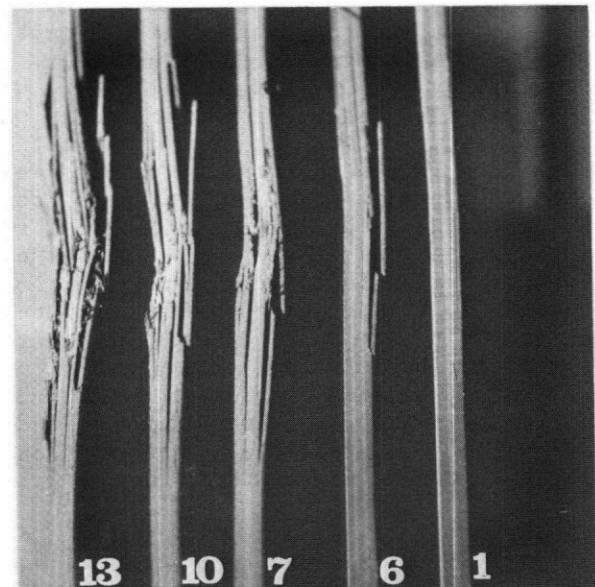


FIG.2- IMPACT TEST DAMAGE ON SMALL SPECIMENS AND PHOTOMICROGRAPHS OF SPECIMEN 1.

3. C-scan Ultrasonic Test Method

Specimens were inspected by pulse echo ultrasonic in immersion with a C-scan visualization of the signal. The output US signal is measured in amplitude and converted by an A/D circuit to 16 colours corresponding each to a value of acoustic pressure. A transducer focalized on one point was used to obtain better signal/noise ratio; in such way defects are displayed with high sensibility and, furthermore, is possible to examine the defect in each layer. A 15 MHz transducer was used to inspect panels. The transducer was, for first, characterized to obtain the true beam profile, DAC curves and signal analysis; furthermore, since the small thickness of laminates, a broad band transducer highly damped was used. Afterwards, the ultrasonic equipment was calibrated by using a laminated specimen including some teflon layers to simulate delaminations at different distance from the surface. Since focalized transducers analyze a thickness equal to the focal length, the maximum focal distance of the material was evaluated for first and then the distance between the transducer and the laminate surface.

4. Buckling Analysis of Anisotropic Plates

An analytical solution was developed for the buckling of anisotropic cylindrical plates under biaxial compression and shear loads. Linear equations for laminated cylindrical shells, Donnell-type equations, are used in conjunction with Galerkin's method to determine critical buckling loads. For many engineering applications of curved plates, the ratios of radius of curvature to plate thickness are often greater than 500; hence, Donnell's theory should provide sufficient accuracy. Furthermore, the ratio of inplane dimensions to thickness will be greater than 40; in such cases shear deformation will not be significant for practical laminate; thus, in a first stage, the shear deformation is not included in the buckling analysis. The plate thickness is denoted by h , the radius of curvature by R and the in plane dimensions by a and b ; the plate is composed of an arbitrary number of layers with arbitrary fibre orientation in each layer. Based on the Classical Lamination Theory, the following plate equations of equilibrium, in nondimensional form, have been used:

$$L_{11}U + L_{12}V + L_{13}W = 0 ; L_{12}U + L_{22}V + L_{23}W = 0 ; \quad (1)$$

$$L_{13}U + L_{23}V + L_{33}W = N_{\zeta}W_{,\zeta\zeta} + 2A N_{\zeta\eta}W_{,\zeta\eta} + A^2 N_{\eta\eta}W_{,\eta\eta} .$$

where the linear operators L_{ij} are function of the extensional, coupling and bending

stiffnesses of the laminate as well as of the geometric dimension of the curved panels ($g_{\zeta\zeta}$); U, V and W are the displacements of the middle surface in the ζ, η and z directions; N_{ζ}, N_{η} and $N_{\zeta\eta}$ denote the prebuckled average axial, transverse and shear loads per unit width. Both the simply supported (BC-1) and fully clamped (BC-3) boundary conditions are taken into consideration; the following conditions are to be satisfied:

$$\begin{aligned} \text{BC-1:} \quad & \text{at } \zeta=0,1 : N_{\zeta} = M_{\zeta} = V = W = 0 ; \\ & \text{at } \eta=0,1 : N_{\eta} = M_{\eta} = U = W = 0 \end{aligned} \quad (2)$$

$$\begin{aligned} \text{BC-3:} \quad & \text{at } \zeta=0,1 : U = V = W = W_{,\zeta} = 0 ; \\ & \text{at } \eta=0,1 : U = V = W = W_{,\eta} = 0 \end{aligned}$$

A solution of the problem was assumed to be in the well known form:

$$U = \sum_m \sum_n A_{mn} \phi_{mn}(\zeta, \eta) ; V = \sum_m \sum_n B_{mn} \chi_{mn}(\zeta, \eta)$$

$$W = \sum_m \sum_n C_{mn} \psi_{mn}(\zeta, \eta) . \quad (3)$$

The following functions were used for the two sets:

$$\begin{aligned} \text{BC-1)} \quad & \phi_{mn} = \cos m\pi\zeta \sin n\pi\eta ; \chi_{mn} = \sin m\pi\zeta \cos n\pi\eta \\ & \psi_{mn} = \sin m\pi\zeta \sin n\pi\eta ; \end{aligned} \quad (4)$$

$$\text{BC-3)} \quad \phi_{mn} = \chi_{mn} = \sin m\pi\zeta \sin n\pi\eta ; \psi_{mn} = X_m(\zeta) Y_n(\eta)$$

where:

$$X_m(\zeta) = \cosh \gamma_m \zeta - \cos \gamma_m \zeta - \alpha_m (\sinh \gamma_m \zeta - \sin \gamma_m \zeta)$$

$$Y_n(\eta) = \cosh \gamma_n \eta - \cos \gamma_n \eta - \alpha_n (\sinh \gamma_n \eta - \sin \gamma_n \eta)$$

are the beam characteristic shape corresponding to a beam clamped on each end.

As derivation of the two sets BC-1 and BC-3, other two boundary conditions were obtained considering two opposite sides clamped and the other two simply supported and viceversa.

The plate equations of equilibrium, with the associated boundary conditions, were solved out by the Galerkin method. The computer program ALPATAR has been developed for working out the set of linear algebraic equations in the form of an eigenvalue problem:

$$[M_{ij}] - \lambda [K_{ij}] \{A_{mn}, B_{mn}, C_{mn}\}^T = [0] \quad (5)$$

Theoretical analysis and computer program have been developed for any unsymmetric and unbalanced laminate. Analytical results on the buckling of flat and cylindrical panels under inplane loads, obtained by the computer program ALPATAR, show the importance of anisotropic stiffnesses on the correct prediction of the critical loads.

That means that is not possible, in the most of the case, to extend to a generic laminate the theoretical analysis of specially orthotropic plates for determining the buckling loads; significant non conservative errors (up to 50%) can occur in comparison with the anisotropic solution. In particular, the buckling load of panels under inplane shear is very much affected by the positive or negative direction of load application.

Furthermore, significant nonconservative errors can occur for the buckling prediction of thick plates (i.e. the ratio of inplane dimension to thickness less than 40) when the transverse shear deformation is not taken into account. A higher order shear deformation theory was performed on flat and cylindrical panels by assuming a parabolic distribution of transverse shear strain through the plate thickness^(5,6). By applying the principle of virtual work has been possible to obtain exact solutions of the governing equation of motion for a simple supported cross ply and antisymmetric angle ply. The first results obtained show as the shear effects on the buckling load are more pronounced as the ratio of the the principal moduli and the numbers of layers increase. For an angle ply laminate $(-45/45)_3$ with a length to thickness ratio of 10 and an E_1/E_2 ratio of 40 a buckling load reduction of 50% will occur in comparison with the CPT.

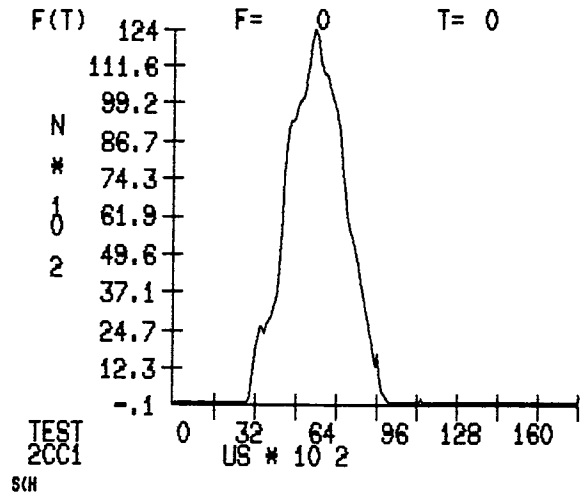
5. Impact Damage on Flat Panels for Buckling Tests

Several experimental tests were carried out on flat panels impacted at different energy levels by the dropped mass test method. Panels were manufactured by using graphite/bismaleimide T800/5245C BASF material laid up at $[45_2/-45_2/0_2/90_2]_{NS}$; all panels were vacuum bagged and autoclave cured. Panels tested under shear load had 16 layers, resulting an average thickness of 2.08 mm, and dimensions of 37 by 23.5 cm; panels tested under compression load had 32 layers, resulting an average thickness of 4.25mm, and dimensions of 42.2 by 25.3 cm. A summary of the impact data are presented in Table 2. Two different mass (1.5 and 2.76 kg) were used to impact panels. Panels number 1 and 2 where clamped between two steel plates having a 4 cm central hole and then impacted; panel number 4, 5, 6 and 2C where clamped between steel rectangular frame of 34.5 by 21 cm inner dimension and then impacted in the centre; panels number 3 and 3C were not imposed to any impact.

A typical response of impact force and energy as function of time is reported in Fig. 3 for panel 2C.

Panel N.	1	2	4	5	6	2C
Velocity [m/sec]	5.5	3.5	5.5	6.5	5.5	6.5
Energy [J]	22	9.1	41	31	22	58

TABLE 2 IMPACT TEST ON FLAT PANELS



ITIS 'C. GRASSI' - TORINO
LABORATORIO DI TECNOLOGIE AERONAUTICHE

PROVA N. 2CC1 MAT. 5245T800
M= 2.757 V= 6.5
DATA 19-09-89
OPERATORE PEGOLO M.

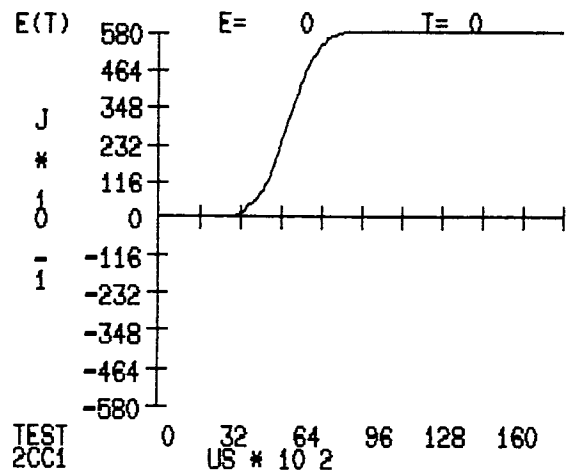


FIG.3- IMPACT FORCE AND ENERGY AS FUNCTION OF TIME FOR PANEL 2C.

Panels were ultrasonically inspected to examine the impact damage; Fig. 4a represents the C-scan of panel 6 as in the overall dimension as well as the magnification of the damaged area (having dimension of 43 by 41 mm). The white area inside the dark damaged area represents the contact zone between the laminate and the impactor; the local deformation induced in the laminate increase the distance between the surface laminate and the transducer; in this zone the

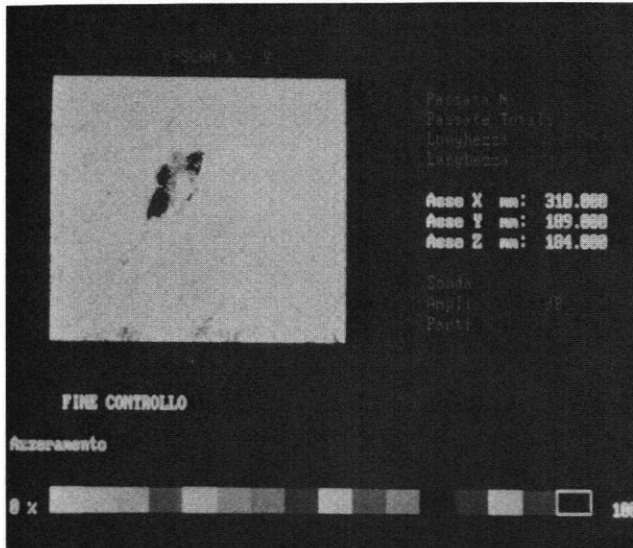


FIG.4a- C-SCAN OF PANEL 6

laminate is out of the focal length and the US signal is attenuated. The different tonalities noted in the picture, corresponding to several acoustic pressure, represent delamination occurred between layers disposed at different distance from the surface. Fig. 4b represents the C-scan of panel 5.

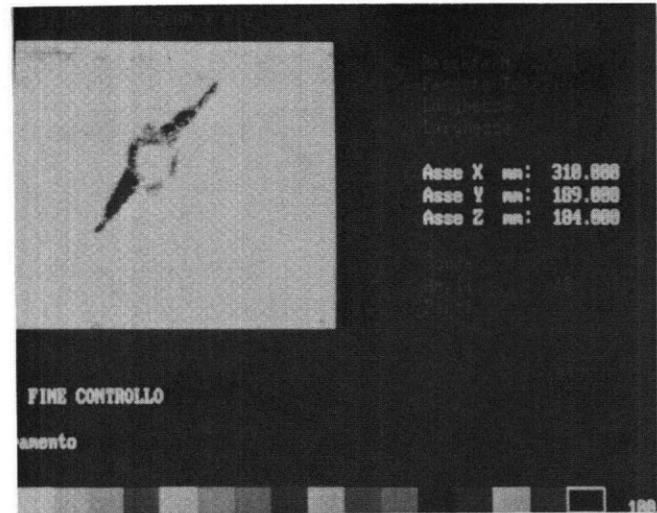


FIG.4b- C-SCAN OF PANEL 5

6. Experimental Results for Panels under Inplane Shear or Compression Load.

Seven panels were tested under inplane shear and two under uniaxial compression to verify the correlation between the preceding theoretical analysis and experimental results looking, in particular, to the effects of impact damage on the buckling behaviour. Material properties used in the analysis were experimentally determined to be: $E_1=142$ GPa; $E_2=5.46$ GPa; $G_{12}= 2.86$ GPa; $\nu_{12}=.3$.

The picture-frame test fixture used for shear tests is composed of two steel rails bolted to the edges of each specimen; the rails are connected with pins which do not extend through the test panels; a tension load, applied along one diagonal, was used to test the specimens; panels were assumed to be simply supported along all edges.

The test fixture used for compression tests provided a clamped boundary condition on the loaded ends and a simply supported boundary condition on the unloaded sides of the panels.

Several strain gages, either linear or rosette, were back to back bonded to panels to measure in plane strain. Out-of-plane displacements were monitored by the shadow moiré method, and fringe patterns were recorded by a camera. The critical load at

which a panel displayed buckling was defined by load-strain curves as the value at which strain reversal occur, together with moiré fringe patterns when clearly developed.

A summary of the results is reported in Table 3. Theoretical analysis reported in paragraph 3 was used to determine the buckling load.

Experimental results obtained for panels under shear tests are reported in Figure 5. The applied load along the diagonal is reported as function of different back to back strain gages; strains obtained by rosettes were worked out to obtain principal strains; however, strains measured by the 45° gages, quasi perpendicular to applied load, are reported in the pictures, since they display the buckling load too. Results for panel 3, not impacted, are reported in Fig.5a and 5b; a positive shear was first applied up to 32.5 kN; then, after removing the load, a negative shear was applied up to the failure load; it is very clear, from the pictures, the great difference in buckling loads, as it was analytically predicted by ALPATAR computer program. Panel 3 carried a high load in the postbuckling range and failure occurred by an explosive delamination having reached the maximum fibre compression strain.

Panel	Test	Theoret. Buckling Load [kN]	Experimental Load	
			Buckling [kN]	Failure [kN]
3	Shear +	30.59(*)	30	No Fail
3	Shear -	19.91(*)	20	77
1	Shear +		27.5	70
2	Shear -		15	77
4	Shear -		14	66
5	Shear +		25	69
6	Shear +		24	No Fail
3C	Compres	75	75	162
2C	Compres		65	142

(*) $P_{buck} = N_{xy} * b / \cos(57.58)$

TABLE 3 - EXPERIMENTAL RESULTS FOR PANELS UNDER SHEAR AND COMPRESSION LOAD

Panel 1, 5 and 6, tested after impact under positive shear load, showed a slight reduction (up to 20%) of either buckling load and strain (Fig.5c, 5f and 5g); although impact delaminations were greater in the compression direction, damage did not very much affected postbuckling load range.

Panel 2 and 4, tested after impact under negative shear, showed a greater reduction (up to 30%) of either buckling load and strain (Fig.5d and 5e); in both the cases the greater delamination dimension was in the tensile direction.

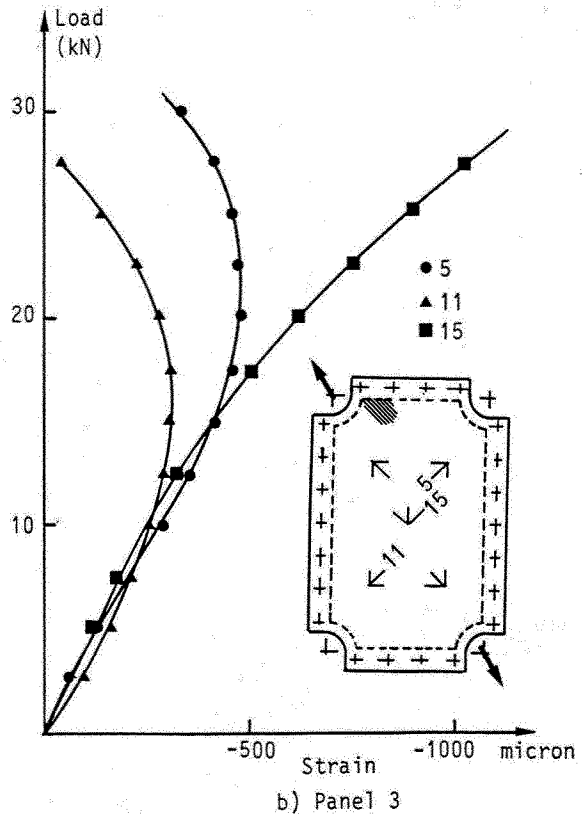
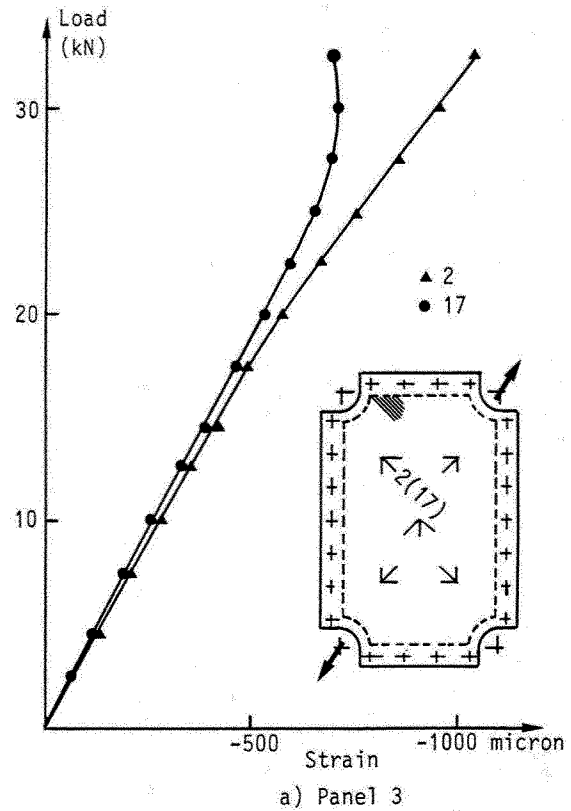
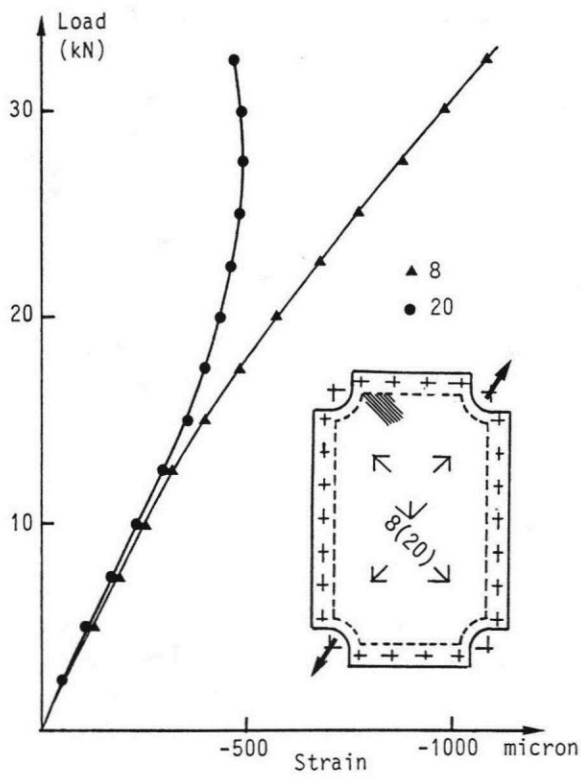
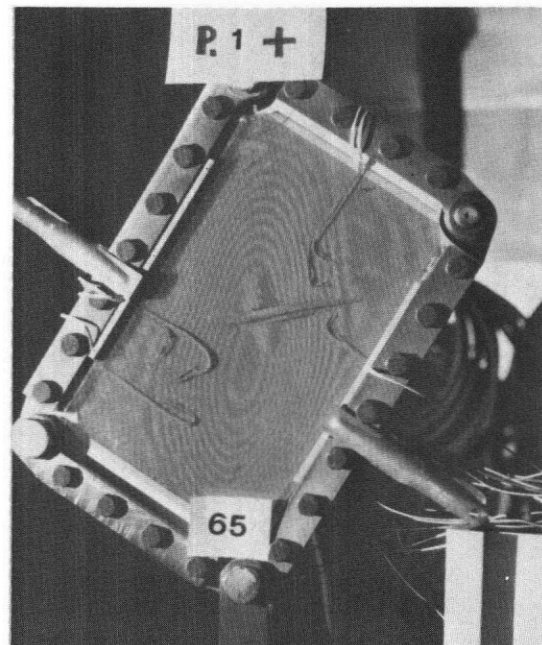
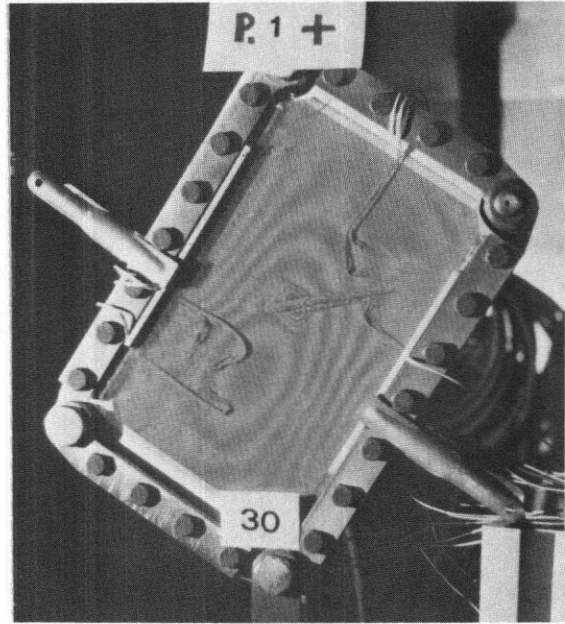
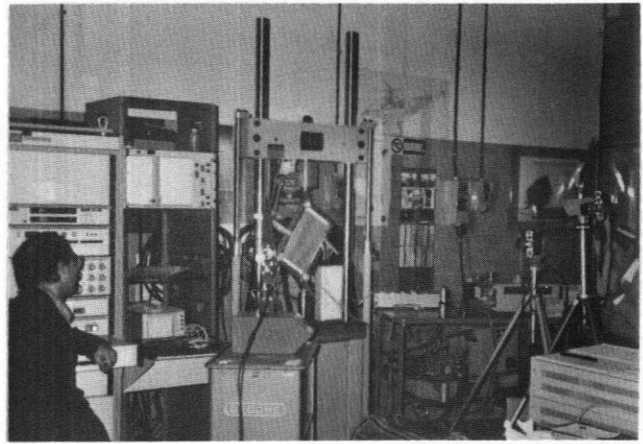
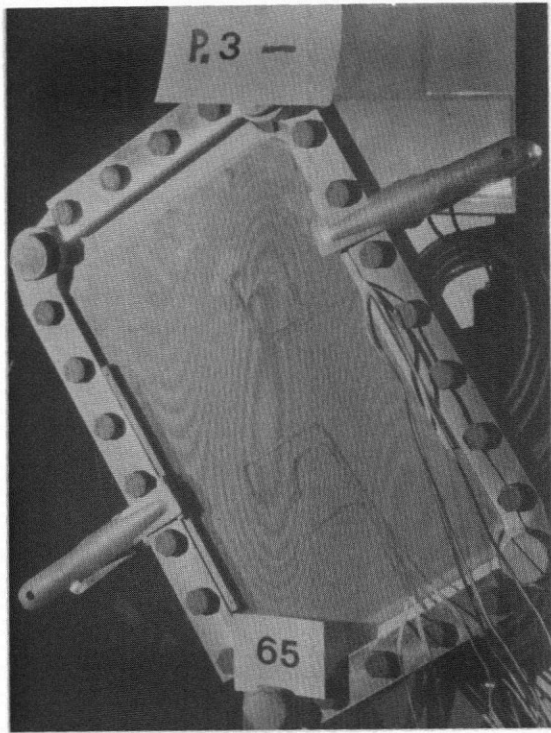


FIG.5- EXPERIMENTAL RESULTS FOR PANELS UNDER SHEAR LOAD.



c) Panel 1

FIG.5- EXPERIMENTAL RESULTS FOR PANELS UNDER SHEAR LOAD. Continue

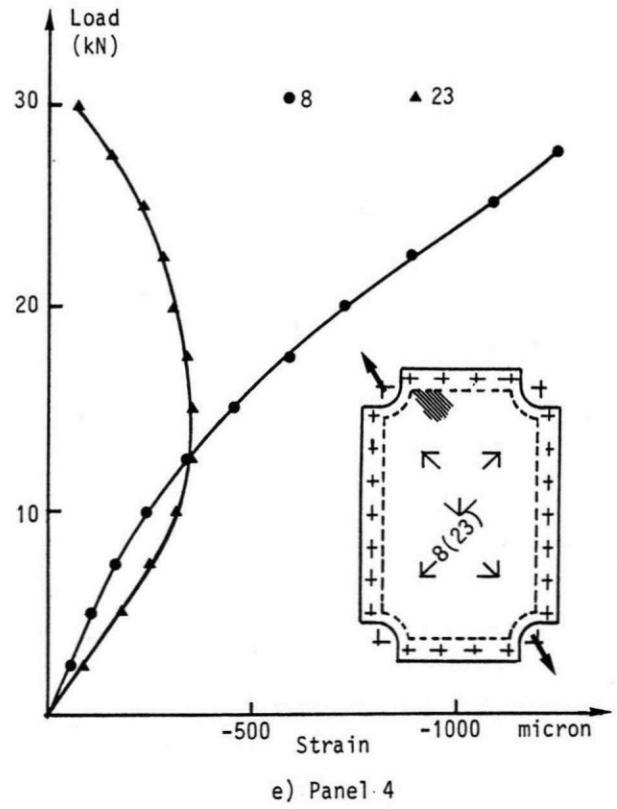
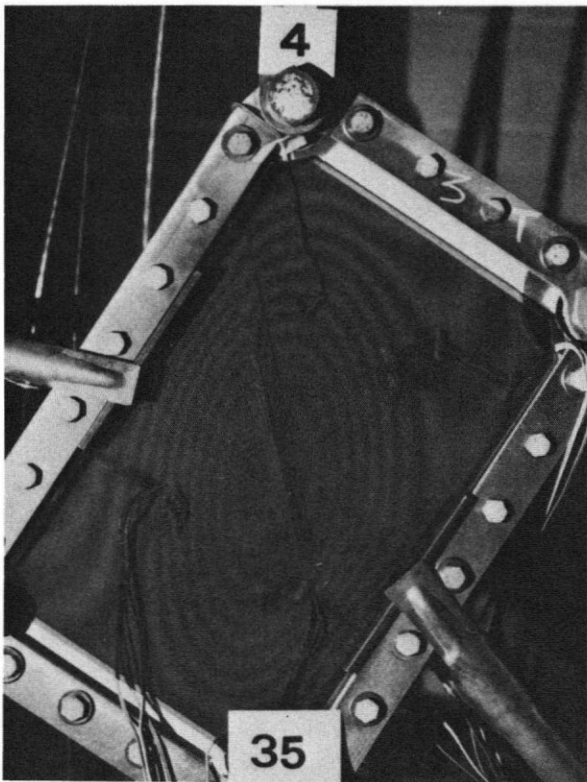
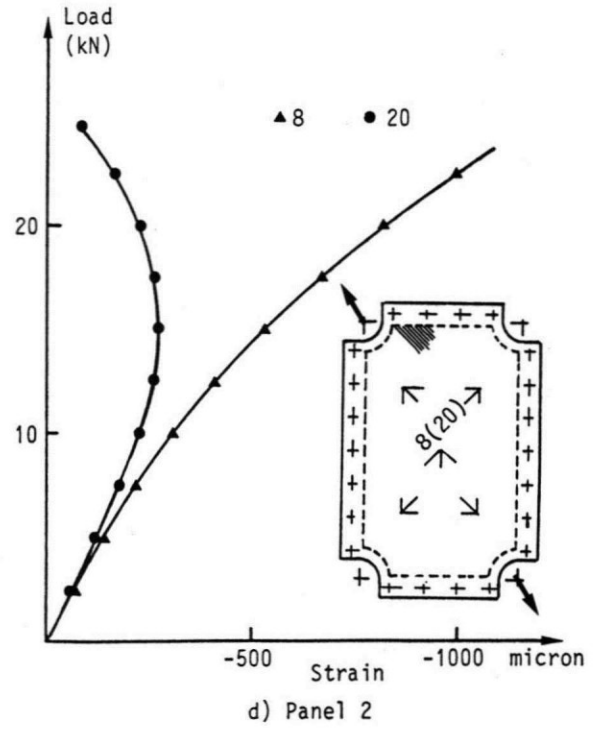
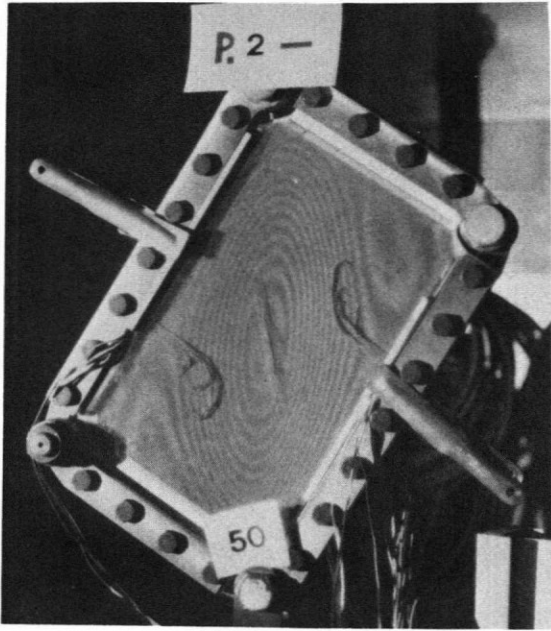


FIG.5- EXPERIMENTAL RESULTS FOR PANELS UNDER SHEAR TEST. Continue

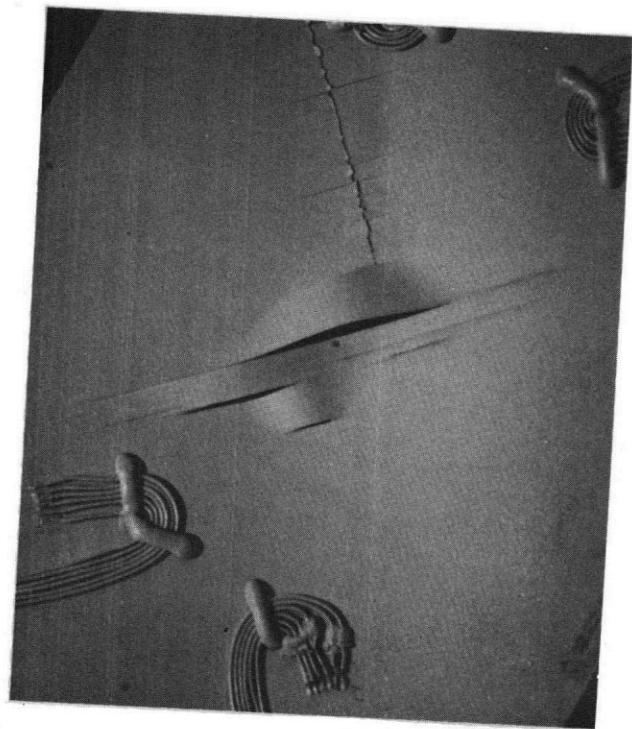
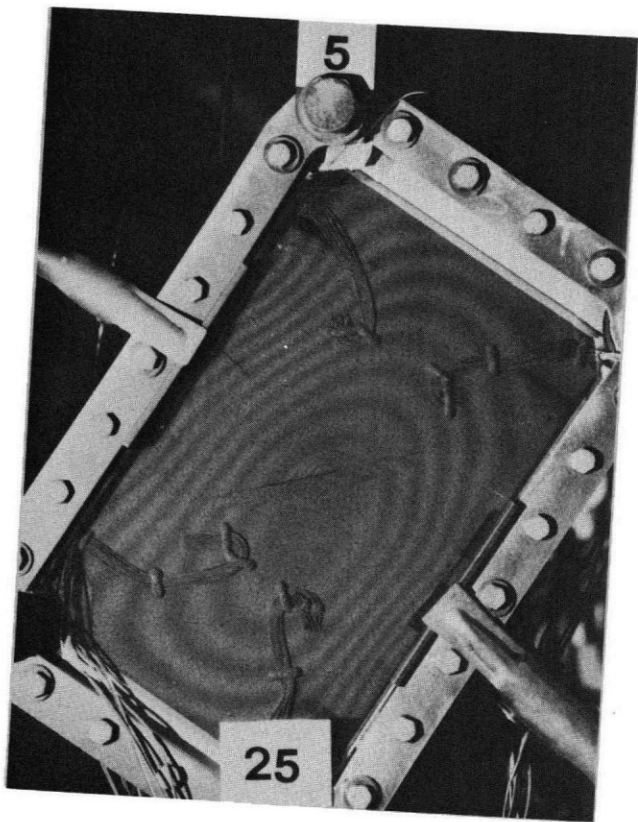
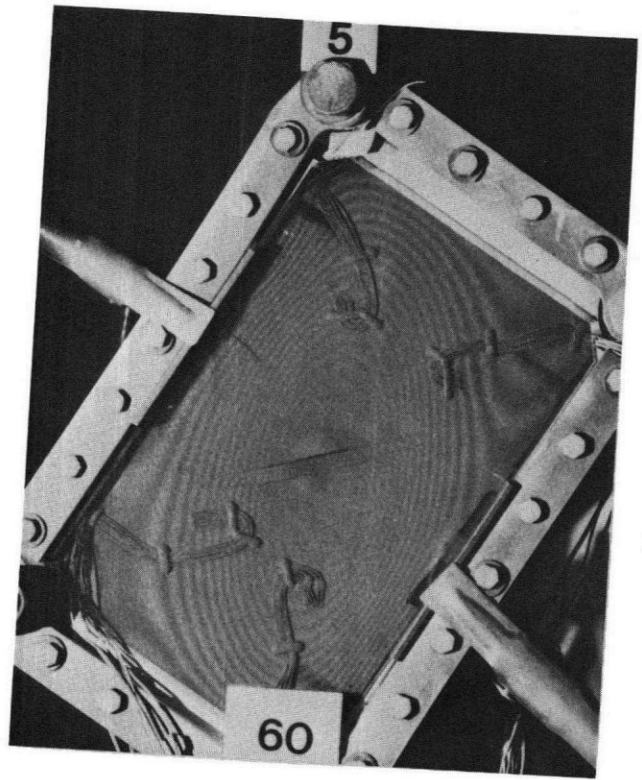
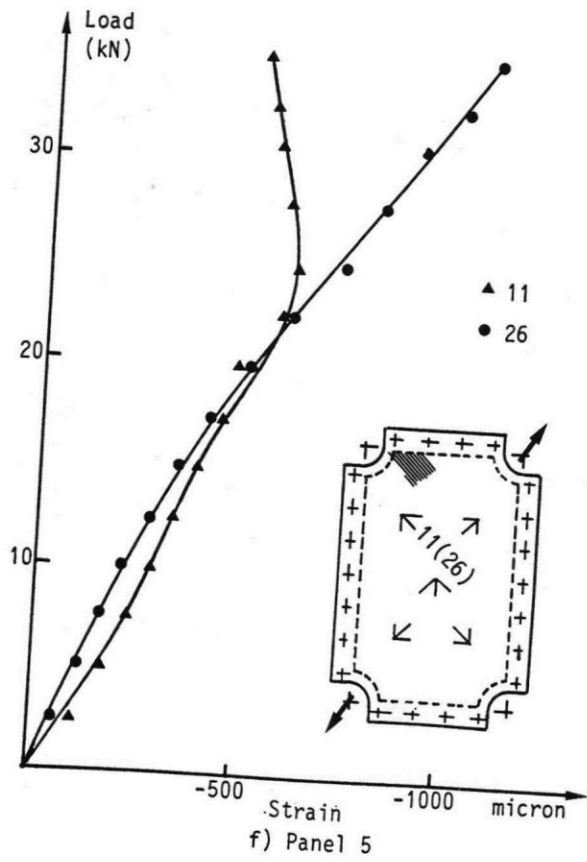


FIG.5- EXPERIMENTAL RESULTS FOR PANELS UNDER SHEAR LOAD.

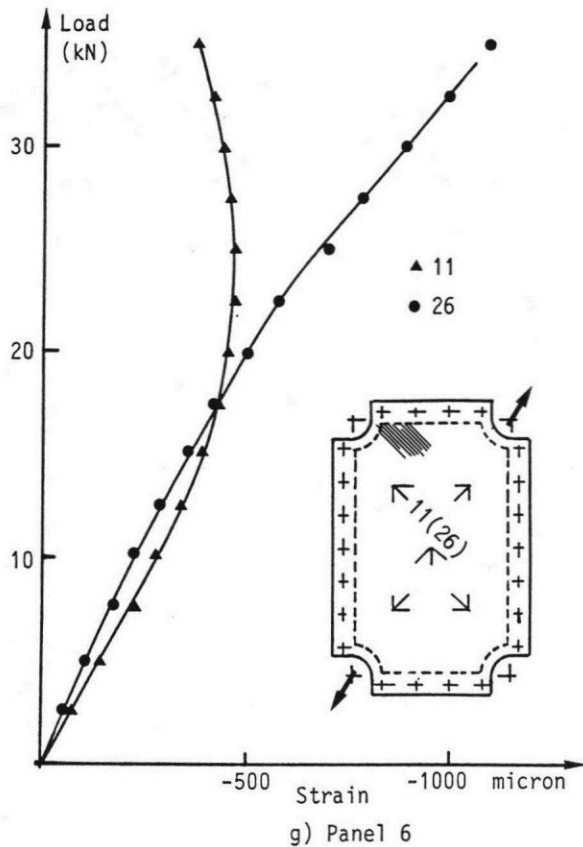


FIG.5- EXPERIMENTAL RESULTS FOR PANELS UNDER SHEAR LOAD. Conclude

Experimental results obtained for panels under uniaxial compression are reported in Fig. 6. The applied load is reported as function of different back to back strain gages disposed either at half length or at a quarter length. Fig. 6a represents the behaviour of the non impacted panel 3C; buckling occurred by two half-waves at a load of 75 kN corresponding exactly to the theoretical value obtained by ALPATAR computer program. Fig. 6b represents the behaviour of the impacted panel 2C; buckling occurred at a load 15% lower that of the non impacted panel; however, an higher strain reduction (up to 50%) was noted in the area around the impact damage (strain gages number 2 and 8) resulting in a lower failure load of the panel.

7. Conclusion

Test results for composite panels under shear or uniaxial compression load correlate well with theory when anisotropic bending stiffnesses are adequately considered. Tests results, however, also show that low velocity impact can cause local delamination and intraply cracking of

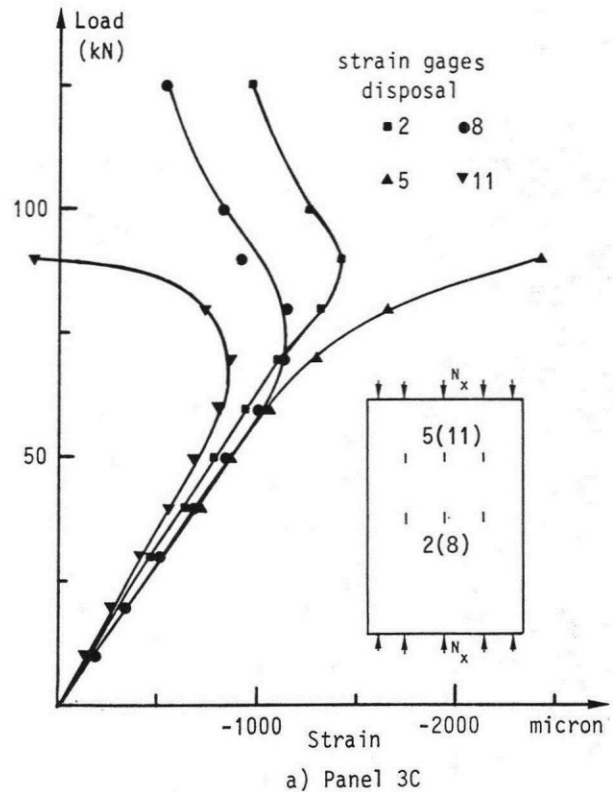
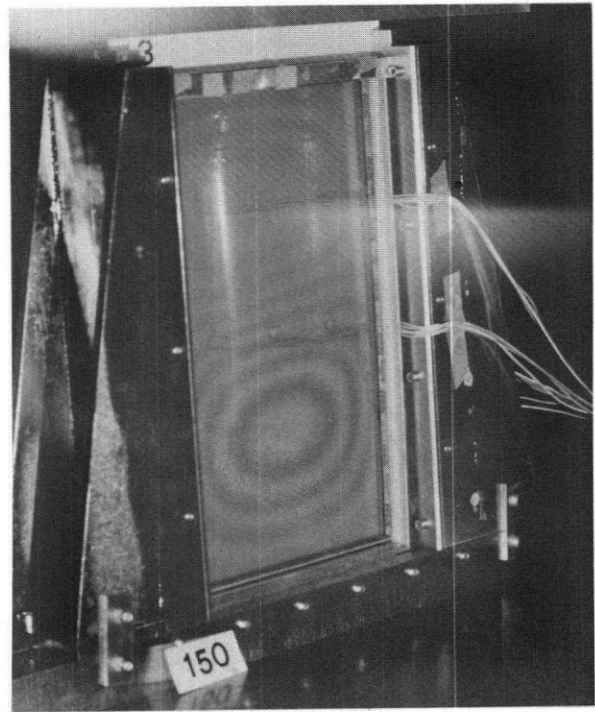


FIG.6- EXPERIMENTAL RESULT FOR PANELS UNDER UNIAXIAL COMPRESSION. Continue

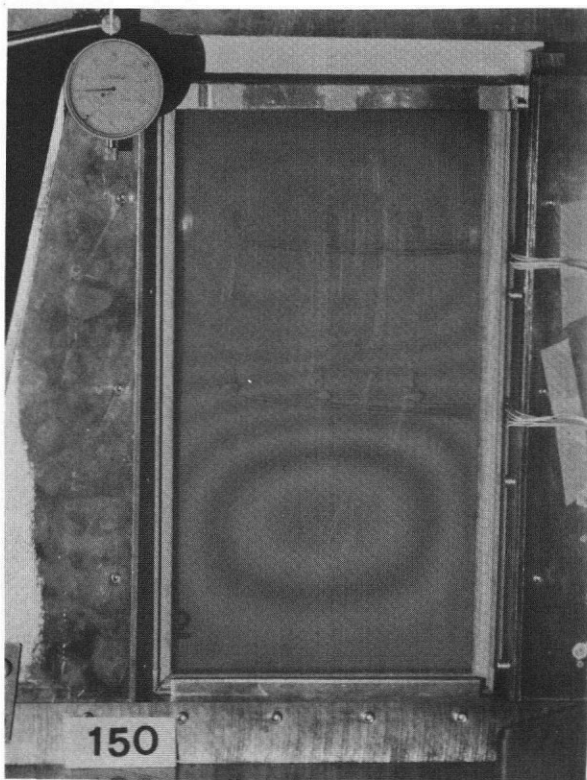
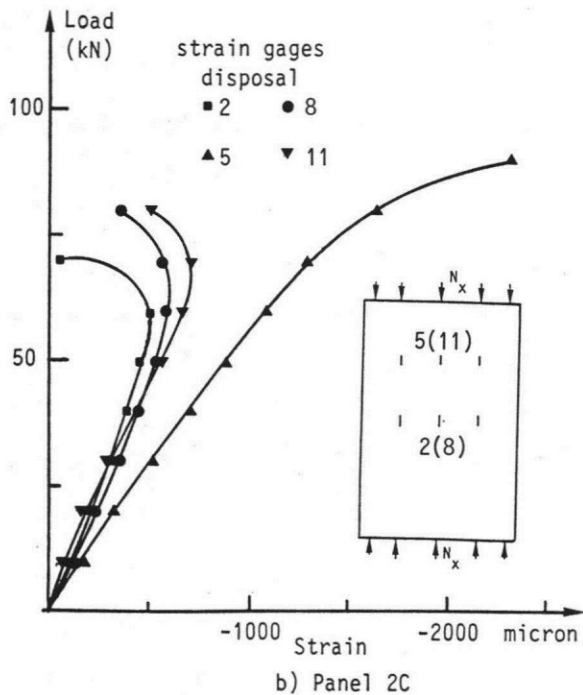


FIG.6- EXPERIMENTAL RESULTS FOR PANELS UNDER UNIAXIAL COMPRESSION. Conclude

the laminate reducing the buckling load and strength of panels. Although significant mass savings can still be achieved by imposing strains lower than are usually applied to metals, the need exists to improve the damage tolerance of composite structures.

8. References

1. Williams J.G. & al 1979, Recent developments in the design, testing and impact damage tolerance of stiffened composite panels, Nasa TM 80077.
2. Williams J.G. & al 1984, Comparison of toughened composite laminates using NASA standard damage tolerance tests, Proc. ACEE Composite Structures Technology Conf., Seattle, USA, CP 2321, 51-73.
3. Whitney J M 1984, Buckling of anisotropic laminated cylindrical plates, AIAA Journal, 22, 11, 1641-1645.
4. Romeo G & al 1989, Stabilità elastica di pannelli curvi anisotropi ed incastrati soggetti a carichi di compressione biassiale e taglio, Proc. 10th Nat. Congress AIDAA (Italian Ass. of Aeron. & Astron.), Pisa, Italy, 9 p.
5. Romeo G & al 1990, Buckling of laminated cylindrical plates including effects of shear deformation, Proc. Int. Symp. Space Application of Advanced Structural Materials, ESA-ESTEC, Noordwijk, NL, 6 p.
6. Reddy J N & Liu C F 1985, A higher-order shear deformation theory of laminated elastic shells, Int. J. Engng Sci, 23, 3, 319-330.